# Coordination and Decentralized Cooperation of Multiple Mobile Manipulators

**O. Khatib,* K. Yokoi, K. Chang, D. Ruspini, R. Holmberg, and A. Casal**
*Robotics Laboratory*
*Department of Computer Science*
*Stanford University*
*Stanford, CA 94086*

Received May 25, 1996

Mobile manipulation capabilities are key to many new applications of robotics in space, underwater, construction, and service environments. This article discusses the ongoing effort at Stanford University for the development of multiple mobile manipulation systems and presents the basic models and methodologies for their analysis and control. This work builds on four methodologies we have previously developed for fixed-base manipulation: the Operational Space Formulation for task-oriented robot motion and force control; the Dextrous Dynamic Coordination of Macro/Mini structures for increased mechanical bandwidth of robot systems; the Augmented Object Model for the manipulation of objects in a robot system with multiple arms; and the Virtual Linkage Model for the characterization and control of internal forces in a multi-arm system. We present the extension of these methodologies to mobile manipulation systems and propose a new decentralized control structure for cooperative tasks. The article also discusses experimental results obtained with two holonomic mobile manipulation platforms we have designed and constructed at Stanford University. 

モービル・マニピュレータの能力は、宇宙空間、水中、建設、運搬の環境におけるロボットとの数多くの新しいアプリケーションにとって重要である。この発表では、現在スタンフォード大学で進められている複合モービル・マニピュレーション・システムの開発について考察し、これらの解析と制御を行うために必要な基本モデルと方法について説明する。この作業

*To whom all correspondence should be addressed.

Journal of Robotic Systems 13(11), 755–764 (1996)

CCC 0741-2223/96/011755-10

では、我々が以前に固定ベースのマニピュレーション・システム用に開発した4つの方法を、モービル・マニピュレータ用に再構築する。4つの方法とは、タスク指向のロボット動作と力の制御を行うための Operational Space Formulation、ロボット・システムの機械的帯域幅を増強する Dextrous Dynamic Coordination of Macro/Mini 構造、複数のアームを持ったロボット・システムで物体の操作を行うための Augmented Object Model、マルチアーム・システムにおける内力の特性化と制御を行う Virtual Linkage Model である。そして、ここでは、これら4つの方法のモービル・マニピュレーション・システムへの拡張について説明し、協調作業に関する新しい分散制御構造を提案する。また、この発表では、スタンフォード大学で設計して組み立てた2台の完全なモービル・マニピュレーション・プラットフォームを使った実験結果についても考察する。

## 1. INTRODUCTION

A central issue in the development of mobile manipulation systems is vehicle/arm coordination. This area of research is relatively new. There is, however, a large body of work that has been devoted to the study of motion coordination in the context of kinematic redundancy. In recent years, these two areas have begun to merge, and algorithms developed for redundant manipulators are being extended to mobile manipulation systems.[1–4]

Typical approaches to motion coordination of redundant systems involve the use of pseudo- or generalized inverses to solve an under-constrained or degenerate system of linear equations, while optimizing some given criterion. These algorithms are essentially driven by kinematic considerations, and the dynamic interaction between the end effector and the manipulator's internal motions are ignored.

Our approach to controlling redundant systems is based on two models: an *end-effector dynamic model*[5] obtained by projecting the mechanism dynamics into the operational space, and a *dynamically consistent force/torque relationship*[6] that provides decoupled control of joint motions in the null space associated with the redundant mechanism. These models form the basis for the dynamic coordination strategy we are implementing on the mobile manipulation platforms. With this strategy, the vehicle/arm system can be viewed as the mechanism resulting from the serial combination of two sub-systems: a "macro" structure with coarse, slow, dynamic responses (the mobile base), and a relatively fast and accurate "mini" device (the manipulator).

Another important issue in mobile manipulation concerns cooperative operations between multiple vehicle/arm systems.[7–11] An example of cooperative operations involving multiple vehicle/arm systems in construction tasks is illustrated in Figure 1. Our research in cooperative manipulation has produced a number of results that provide the basis for the control strategies we are developing for mobile manipulation platforms. Our approach is based on the integration of two basic concepts: The *augmented object*[12] and the *virtual linkage*.[13] The *virtual linkage* characterizes internal forces, while the *augmented object* describes the system's closed-chain dynamics. These models have been successfully used in cooperative manipulation for various compliant motion tasks performed by two and three PUMA 560 manipulators.[14]

The *augmented object* model we developed for fixed base multi-arm robots has been extended to the multiple vehicle/arm systems. The dynamics at the operational point of a multiple vehicle/arm system are described by an *augmented object* model, which is obtained by combining the dynamics of the individual mobile manipulators and the object. Control of this highly redundant system relies on both the *dynamically consistent* relationships between joint forces and end-effector forces for each mobile arm.

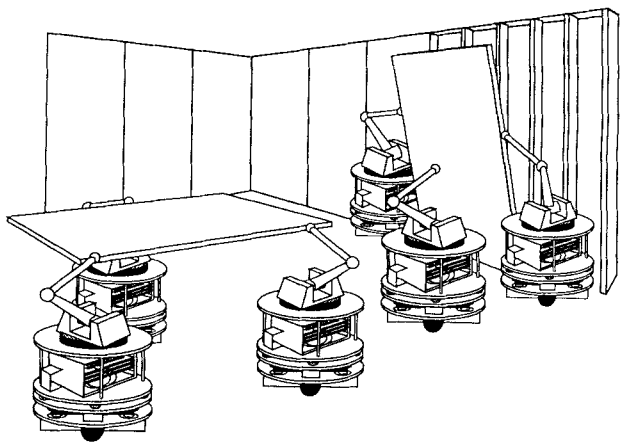

**Figure 1.** A construction task: Drywall.

While providing an accurate description of cooperative manipulation, the *augmented object* and *virtual linkage* models have been implemented in an architecture that requires some level of centralized control, which is not quite suited for autonomous mobile manipulation platforms. The article presents a new strategy based on the *augmented object* and *virtual linkage* models for decentralized cooperative operations between multiple mobile manipulation platforms.

## 2. VEHICLE/ARM COORDINATION

### 2.1. Dynamics

The joint space dynamics of a manipulator are described by

$$A(\mathbf{q})\ddot{\mathbf{q}} + \mathbf{b}(\mathbf{q}, \dot{\mathbf{q}}) + \mathbf{g}(\mathbf{q}) = \Gamma; \tag{1}$$

where $\mathbf{q}$ is the $n$ joint coordinates and $A(\mathbf{q})$ is the $n \times n$ kinetic energy matrix. $\mathbf{b}(\mathbf{q}, \dot{\mathbf{q}})$ is the vector of centrifugal and Coriolis joint-forces and $\mathbf{g}(\mathbf{q})$ is the gravity joint-force vector. $\Gamma$ is the vector of generalized joint-forces.

The operational space equations of motion of a manipulator are[5]

$$\Lambda(\mathbf{x})\ddot{\mathbf{x}} + \mu(\mathbf{x}, \dot{\mathbf{x}}) + \mathbf{p}(\mathbf{x}) = \mathbf{F}; \tag{2}$$

where $\mathbf{x}$ is the vector of the $m$ operational coordinates describing the position and orientation of the effector, $\Lambda(\mathbf{x})$ is the $m \times m$ kinetic energy matrix associated with the operational space. $\mu(\mathbf{x}, \dot{\mathbf{x}})$, $\mathbf{p}(\mathbf{x})$, and $\mathbf{F}$ are, respectively, the centrifugal and Coriolis force vector, gravity force vector, and generalized force vector acting in operational space.

### 2.2. Redundancy

The operational space equations of motion describe the dynamic response of a manipulator to the application of an operational force $\mathbf{F}$ at the end effector. For non-redundant manipulators, the relationship between operational forces, $\mathbf{F}$, and joint forces, $\Gamma$ is

$$\Gamma = J^T(\mathbf{q})\mathbf{F}; \tag{3}$$

where $J(\mathbf{q})$ is the Jacobian matrix.

However, this relationship becomes incomplete for redundant systems. We have shown that the relationship between joint torques and operational forces is

$$\Gamma = J^T(\mathbf{q})\mathbf{F} + [I - J^T(\mathbf{q})\bar{J}^T(\mathbf{q})]\Gamma_0; \tag{4}$$

with

$$\bar{J}(\mathbf{q}) = A^{-1}(\mathbf{q})J^T(\mathbf{q})\Lambda(\mathbf{q}); \tag{5}$$

where $\bar{J}(\mathbf{q})$ is the *dynamically consistent generalized inverse*.[6] This relationship provides a decomposition of joint forces into two dynamically decoupled control vectors: joint forces corresponding to forces acting at the end effector ($J^T\mathbf{F}$); and joint forces that only affect internal motions, ($[I - J^T(\mathbf{q})\bar{J}^T(\mathbf{q})]\Gamma_0$).

Using this decomposition, the end effector can be controlled by operational forces, whereas internal motions can be independently controlled by joint forces that are guaranteed not to alter the end effector's dynamic behavior. This relationship is the basis for implementing the dynamic coordination strategy for a vehicle/arm system.

The end-effector equations of motion for a redundant manipulator are obtained by the projection of the joint-space equations of motion (1), by the *dynamically consistent* generalized inverse $\bar{J}^T(\mathbf{q})$,

$$\begin{aligned} &\bar{J}^T(\mathbf{q})[A(\mathbf{q})\ddot{\mathbf{q}} + \mathbf{b}(\mathbf{q}, \dot{\mathbf{q}}) + \mathbf{g}(\mathbf{q}) = \Gamma] \\ &\Rightarrow \Lambda(\mathbf{q})\ddot{\mathbf{x}} + \mu(\mathbf{q}, \dot{\mathbf{q}}) + \mathbf{p}(\mathbf{q}) = \mathbf{F}; \end{aligned} \tag{6}$$

The above property also applies to non-redundant manipulators, where the matrix $\bar{J}^T(\mathbf{q})$ reduces to $J^{-1}(\mathbf{q})$.

### 2.3. Inertial Property

A mobile manipulator system can be viewed as the mechanism resulting from the serial combination of two sub-systems: a "macro" mechanism with coarse, slow, dynamic responses (the mobile base), and a relatively fast and accurate "mini" device (the manipulator).

The mobile base referred to as the *macro structure* is assumed to be holonomic. Let $\Lambda$ be the *pseudo kinetic energy matrix* associated with the combined macro/mini structures and $\Lambda_m$ the operational space *kinetic energy matrix* associated with the mini structure alone.

The magnitude of the inertial properties of macro/mini structure in a direction represented by a unit vector $\mathbf{w}$ in the $m$-dimensional space can be

described by the scalar[6]

$$\sigma_w(\Lambda) = \frac{1}{(\mathbf{w}^T\Lambda^{-1}\mathbf{w})};$$

which represents the effective inertial properties in the direction $\mathbf{w}$.

Our study has shown[6] that, *in any direction* $\mathbf{w}$, *the inertial properties of a macro/mini-manipulator system are smaller than or equal to the inertial properties associated with the mini-manipulator in that direction:*

$$\sigma_w(\Lambda) \leq \sigma_w(\Lambda_m). \tag{7}$$

A more general statement of this *reduced effective inertial* property is that the inertial properties of a redundant system are bounded above by the inertial properties of the structure formed by the smallest distal set of degrees of freedom (DOF) that span the operational space.

### 2.4. Coordination Strategy

The reduced effective inertial property shows that the dynamic performance of a combined macro/mini system can be made comparable to (and, in some cases, better than) that of the lightweight mini manipulator. The idea behind our approach for the coordination of macro and mini structures is to treat them as a single redundant system. High dynamic performance for the manipulated object task (motion and contact forces) can be achieved with an operational space control system using essentially the fast dynamic response of the mini structure.[4] However, given the mechanical limits on the mini structure's joint motions, this would rapidly lead to joint saturation of the mini-structure degrees of freedom.

The *dynamic coordination* we propose is based on combining the operational space control with a minimization of deviation from the midrange joint positions of the mini-manipulator. This minimization must be implemented with joint force control vectors selected from the *dynamically consistent* null space of equation (4). This will eliminate any effect of the additional control forces on the end-effector task.

Let $\bar{q}_i$ and $\underline{q}_i$ be the upper and lower bounds on the $i^{\text{th}}$ joint position $q_i$. We construct the potential function

$$V_{\text{coordination}}(\mathbf{q}) = k_c \sum_{i=n_M+1}^{n} \left(q_i - \frac{\bar{q}_i + \underline{q}_i}{2}\right)^2; \tag{8}$$

where $k_c$ is a constant gain and $n_M$ is the macro structure's number of dof. The gradient of this function

$$\boldsymbol{\Gamma}_{\text{coordination}} = -\nabla V_{\text{coordination}}; \tag{9}$$

provides the required attraction to the mid-range joint positions of the mini-manipulator. The interference of these additional forces with the end-effector dynamics is avoided by projecting them into the null space of $J^T(\mathbf{q})$. This is

$$\boldsymbol{\Gamma}_{\text{null-space}} = [I - J^T(\mathbf{q})\bar{J}^T(\mathbf{q})]\boldsymbol{\Gamma}_{\text{coordination}}. \tag{10}$$

In addition, joint limit avoidance can be achieved using an "artificial potential" function.[15]

## 3. COOPERATIVE MANIPULATION

### 3.1. Augmented Object

The *augmented object* model provides a description of the dynamics at the operational point for a multi-arm robot system. The simplicity of these equations is the result of an additive property that allows us to obtain the system equations of motion from the equations of motion of the individual mobile manipulators.

The *augmented object* model is

$$\Lambda_\oplus(\mathbf{x})\ddot{\mathbf{x}} + \mu_\oplus(\mathbf{x}, \dot{\mathbf{x}}) + \mathbf{p}_\oplus(\mathbf{x}) = \mathbf{F}_\oplus; \tag{11}$$

with

$$\Lambda_\oplus(\mathbf{x}) = \Lambda_{\mathcal{O}}(\mathbf{x}) + \sum_{i=1}^{N} \Lambda_i(\mathbf{x}); \tag{12}$$

where $\Lambda_{\mathcal{O}}(\mathbf{x})$ and $\Lambda_i(\mathbf{x})$ are the kinetic energy matrices associated with the object and the $i^{\text{th}}$ effector, respectively. The vector, $\mu_\oplus(\mathbf{x}, \dot{\mathbf{x}})$ of centrifugal and Coriolis forces also has the additive property

$$\mu_\oplus(\mathbf{x}, \dot{\mathbf{x}}) = \mu_{\mathcal{O}}(\mathbf{x}, \dot{\mathbf{x}}) + \sum_{i=1}^{N} \mu_i(\mathbf{x}, \dot{\mathbf{x}}); \tag{13}$$

where $\mu_{\mathcal{O}}(\mathbf{x}, \dot{\mathbf{x}})$ and $\mu_i(\mathbf{x}, \dot{\mathbf{x}})$ are the vectors of centrifugal and Coriolis forces associated with the object and the $i$th effector, respectively. Similarly, the gravity vector is

$$\mathbf{p}_\oplus(\mathbf{x}) = \mathbf{p}_{\mathcal{O}}(\mathbf{x}) + \sum_{i=1}^{N} \mathbf{p}_i(\mathbf{x}); \tag{14}$$

where $\mathbf{p}_{\mathcal{O}}(\mathbf{x})$ and $\mathbf{p}_i(\mathbf{x})$ are the gravity vectors associated with the object and the $i^{th}$ effector. The generalized operational forces $\mathbf{F}_{\oplus}$ are the resultant of the forces produced by each of the $N$ effectors at the operational point.

$$\mathbf{F}_{\oplus} = \sum_{i=1}^{N} \mathbf{F}_i. \tag{15}$$

### 3.2. Virtual Linkage

Object manipulation requires accurate control of internal forces. Recently, we have proposed the *virtual linkage*[13] as a model of internal forces associated with multi-grasp manipulation. In this model, grasp points are connected by a closed, non-intersecting set of virtual links (Fig. 2.) In the case of an $N$-grasp manipulation task, a *virtual linkage* model is a $6(N-1)$ degree of freedom (DOF) mechanism that has $3(N-2)$ linearly actuated members and $N$ spherically actuated joints. Forces and moments applied at the grasp points of this linkage will cause forces and torques at its joints. We can independently specify internal forces in the $3(N-2)$ members, along with $3N$ internal moments at the spherical joints. Internal forces in the object are then characterized by these forces and torques in a physically meaningful way.

The relationship between applied forces, their resultant and internal forces is

$$\begin{bmatrix} \mathbf{F}_{res} \\ \mathbf{F}_{int} \end{bmatrix} = \mathbf{G} \begin{bmatrix} \mathbf{f}_1 \\ \cdot \\ \cdot \\ \cdot \\ \mathbf{f}_N \end{bmatrix}; \tag{16}$$

where $\mathbf{F}_{res}$ represents the resultant forces at the operational point, $\mathbf{F}_{int}$ the internal forces, and $\mathbf{f}_i$ the forces applied at the grasp point $i$. $\mathbf{G}$ is called the grasp description matrix, and relates forces applied at each grasp to the resultant and internal forces in the object. Furthermore, $\mathbf{G}$ can be written as

$$\mathbf{G} = [\mathbf{G}_1 \mathbf{G}_2 \ . \ . \ . \ \mathbf{G}_N];$$

where each $\mathbf{G}_i$ represents the contribution of the $i$th grasp to the resultant and internal forces felt by the object. Also, $\mathbf{G}_i$ can be further decomposed

$$\mathbf{G}_i = \begin{bmatrix} \mathbf{G}_{res,i} \\ \mathbf{G}_{int,i} \end{bmatrix};$$

where $\mathbf{G}_{res,i}$ is the contribution of $\mathbf{G}_i$ to the resultant forces in the object and $\mathbf{G}_{int,i}$ to the internal ones.

The inverse $\mathbf{G}^{-1}$ provides the forces required at the grasp points to produce the resultant and internal forces acting at the object.

$$\begin{bmatrix} \mathbf{f}_1 \\ \cdot \\ \cdot \\ \cdot \\ \mathbf{f}_N \end{bmatrix} = \mathbf{G}^{-1} \begin{bmatrix} \mathbf{F}_{res} \\ \mathbf{F}_{int} \end{bmatrix}. \tag{17}$$

Similarly, $\mathbf{G}^{-1}$ can be written as

$$\mathbf{G}^{-1} = \begin{bmatrix} \overline{\mathbf{G}}_1 \\ \cdot \\ \cdot \\ \cdot \\ \overline{\mathbf{G}}_N \end{bmatrix};$$

with

$$\overline{\mathbf{G}}_i = [\overline{\mathbf{G}}_{res,i} \quad \overline{\mathbf{G}}_{int,i}];$$

where $\overline{\mathbf{G}}_{res,i}$ represents the part of $\overline{\mathbf{G}}_i$ that correspond to the resultant forces at the object; and the matrix $\overline{\mathbf{G}}_{int,i}$ represents the part corresponding to the internal forces.

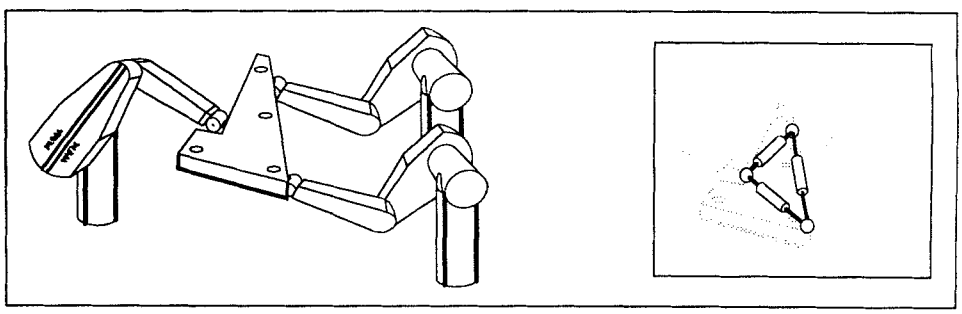

**Figure 2.** The virtual linkage.

### 3.3. Centralized Control Structure

For fixed base manipulation, the *augmented object* and *virtual linkage* have been implemented in a multiprocessor system using a centralized control structure. This type of control is not suited for autonomous mobile manipulation platforms. Before presenting the decentralized implementation, we begin with a brief summary of the centralized control structure.

The overall structure of the centralized implementation is shown in Figure 3. The force sensed at the grasp point of each robot, $\mathbf{f}_{s,i}$, is transformed, via $\mathbf{G}$, to sensed resultant forces $\mathbf{F}_{res,s}$, and sensed internal forces, $\mathbf{F}_{int,s}$, at the operational point, using equation (16)

$$\begin{bmatrix} \mathbf{F}_{res,s} \\ \mathbf{F}_{int,s} \end{bmatrix} = \mathbf{G} \begin{bmatrix} \mathbf{f}_{s,1} \\ \vdots \\ \mathbf{f}_{s,N} \end{bmatrix}.$$

The centralized control strategy strategy consists of (i) a unified motion and force control structure for the *augmented object* corresponding to the resultant force vector, $\mathbf{F}_{res}$; and (ii) a force control vector, $\mathbf{F}_{int}$, corresponding to the internal forces acting on the *virtual linkage*. These are

$$\mathbf{F}_{res} = \mathbf{F}_{motion} + \mathbf{F}_{contact}; \tag{18}$$

where

$$\mathbf{F}_{motion} = \hat{\Lambda}_{\oplus}\Omega\mathbf{F}^{*}_{motion} + \hat{\mu}_{\oplus} + \hat{p}_{\oplus}; \tag{19}$$

$$\mathbf{F}_{contact} = \hat{\Lambda}_{\oplus}\overline{\Omega}\mathbf{F}^{*}_{contact} + \mathbf{F}_{contact,s}. \tag{20}$$

$\hat{\Lambda}_{\oplus}$, $\hat{\mu}_{\oplus}$, and $\hat{p}_{\oplus}$ represent the estimates of $\Lambda_{\oplus}$, $\mu_{\oplus}$, and $\hat{p}_{\oplus}$. The vector $\mathbf{F}^{*}_{motion}$ and $\mathbf{F}^{*}_{contact}$ represent the inputs to the decoupled system. $\Omega$ is the *generalized selection matrix* associated with motion control, and $\overline{\Omega}$, its complement, is associated with force control.

The control structure for internal forces is

$$\mathbf{F}_{int} = \hat{\Lambda}_{\oplus}\mathbf{F}^{*}_{int} + \mathbf{F}_{int,s}; \tag{21}$$

where the vector $\mathbf{F}^{*}_{int}$ represents the inputs to the decoupled system. A suitable control law can be selected to obtain $\mathbf{F}^{*}_{motion}$, $\mathbf{F}^{*}_{contact}$, and $\mathbf{F}^{*}_{int}$.

The control forces of the individual mobile manipulator, $\mathbf{f}_i$, are given by using equation (17),

$$\begin{bmatrix} \mathbf{f}_1 \\ \vdots \\ \mathbf{f}_N \end{bmatrix} = \mathbf{G}^{-1} \begin{bmatrix} \mathbf{F}_{res} \\ \mathbf{F}_{int} \end{bmatrix}.$$

The above strategy has been successfully implemented for two and three PUMA 560 arms.[14]

### 3.4. Decentralized Control Structure

In a multiple mobile robot system, each robot has real-time access only to its own state information, and can only infer information about the other robots' grasp forces through their combined action on the object. In the decentralized control structure we propose, the object level specifications of the task are transformed into individual tasks for each of the cooperative robots. Local feedback control loops are then developed at each grasp point. The task transformation and the design of the local controllers are accomplished in consistency with the *augmented object* and *virtual linkage* models. The overall structure of the proposed decentralized control structure is shown in Figure 4.

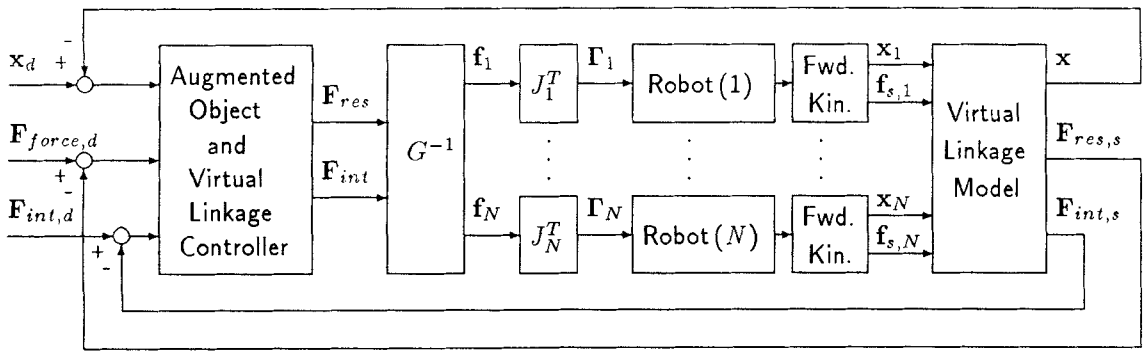


**Figure 3.** Centralized control structure.

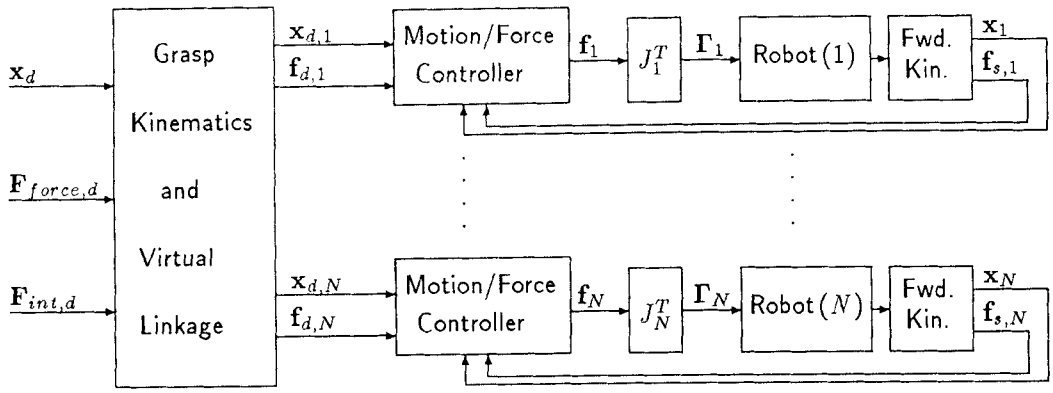


**Figure 4.** Decentralized control structure.

The local control structure at the $i$th grasp point is

$$\mathbf{f}_i = \mathbf{f}_{motion,i} + \mathbf{f}_{force,i}. \tag{22}$$

The control vectors, $\mathbf{f}_{motion,i}$, are designed so that the combined motion of the various $i^{\text{th}}$ grasp points results in the desired motion at the object operational point. On the other hand, the vectors $\mathbf{f}_{force,i}$ create forces at the grasp points, whose combined action produces the desired contact and internal forces on the object.

The motion control at the $i$th grasp point is

$$\mathbf{f}_{motion,i} = \hat{\Lambda}_{\emptyset,i}\Omega\mathbf{f}^*_{motion,i} + \hat{\mu}_{\emptyset,i} + \hat{p}_{\emptyset,i}; \tag{23}$$

with

$$\hat{\Lambda}_{\emptyset,i} = \hat{\Lambda}_{g,i} + \overline{\mathbf{G}}_{res,i}\hat{\Lambda}_{\mathcal{L}}\overline{\mathbf{G}}^T_{res,i}; \tag{24}$$

where $\hat{\Lambda}_{g,i}$ is the kinetic energy matrix associated with the $i^{\text{th}}$ effector at the grasp point. The second term of equation (24) represents the part of $\hat{\Lambda}_{\mathcal{L}}$ assigned to the $i$th robot and described at its grasp point.

The vector, $\hat{\mu}_{\emptyset,i}$, of centrifugal and Coriolis forces associated with the $i^{\text{th}}$ effector is

$$\hat{\mu}_{\emptyset,i} = \hat{\mu}_{g,i} + \overline{\mathbf{G}}_{res,i}\hat{\mu}_{\mathcal{L}}; \tag{25}$$

where $\hat{\mu}_{g,i}$ is the centrifugal and Coriolis vector of the $i$th robot alone at the grasp point. $\overline{\mathbf{G}}_{res,i}\hat{\mu}_{\mathcal{L}}$ represents the part of $\hat{\mu}_{\mathcal{L}}$ assigned to the $i$th robot and described at its grasp point. Similarly, the gravity vector is

$$\hat{p}_{\emptyset,i} = \hat{p}_{g,i} + \overline{\mathbf{G}}_{res,i}\hat{p}_{\mathcal{L}}; \tag{26}$$

where $\hat{p}_{g,i}$ is the gravity vector associated with the $i$th end effector at the grasp point. $\overline{\mathbf{G}}_{res,i}\hat{p}_{\mathcal{L}}$ represents the part of $\hat{p}_{\mathcal{L}}$ assigned to the $i$th robot and described at its grasp point.

The sensed forces at the $i$th grasp point, $\mathbf{f}_{s,i}$, combine the contact and internal forces felt at the $i^{\text{th}}$ grasp point, together with the acceleration force acting at the object. The sensed forces associated with the contact and internal forces alone, $\mathbf{f}_{\bar{s},i}$, are therefore obtained by subtracting the acceleration effect from the total sensed forces

$$\mathbf{f}_{\bar{s},i} = \mathbf{f}_{s,i} - \overline{\mathbf{G}}_{res,i}(\hat{\Lambda}_{\mathcal{L}}\ddot{\mathbf{x}}_d + \hat{\mu}_{\mathcal{L}} + \hat{p}_{\mathcal{L}}). \tag{27}$$

Here, the object desired acceleration has been used instead of the actual acceleration, which would be difficult to evaluate.

The force control part of equation (22) is

$$\mathbf{f}_{force,i} = \hat{\Lambda}_{\emptyset,i}\mathbf{f}^*_{force,i} + \mathbf{f}_{\bar{s},i}; \tag{28}$$

where $\mathbf{f}^*_{force,i}$ represents the input to the decoupled system associated with the contact forces and internal forces. $\mathbf{f}^*_{force,i}$ can be achieved by selecting

$$\mathbf{f}^*_{force,i} = -\mathbf{K}_f(\mathbf{f}_{\bar{s},i} - \mathbf{f}_{d,i}) - \mathbf{K}_{vf}\dot{\mathbf{f}}_{\bar{s},i}. \tag{29}$$

The vector $\mathbf{f}_{d,i}$ is the desired force assigned to the $i$th mobile manipulator. Using equation (17), this vector is

$$\begin{bmatrix} \mathbf{f}_{d,1} \\ \vdots \\ \mathbf{f}_{d,N} \end{bmatrix} = \mathbf{G}^{-1}\begin{bmatrix} \mathbf{F}_{res,d} \\ \mathbf{F}_{int,d} \end{bmatrix}. \tag{30}$$

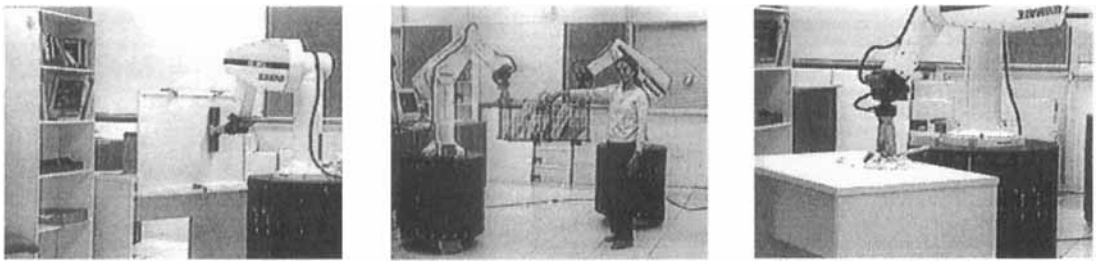

**Figure 5.** Experiments with the mobile platforms. Erasing a whiteboard, cooperating in carrying a basket, and sweeping a desk are examples of tasks demonstrated with the Stanford Mobile Platforms.

where the desired resultant forces are

$$\mathbf{F}_{res,d} = \overline{\Omega}\mathbf{F}_{contact,d}; \tag{31}$$

where $\mathbf{F}_{contact,d}$ is the desired contact force vector.

The assumptions in the above control structure is that the object is rigid and that there is no slippage at the grasp points. Gripper slip in the real system will result in errors in the grasp kinematic computation and inconsistencies with the *virtual linkage* model. To compensate for these effects, some level of communication between the different platforms will be needed for updating the robot state and modifying the task specifications. The rate at which this communication is required is much slower than the local servo control rate. Such communication can be achieved over a radio Ethernet link (at 10–20 Hz).

## 4. EXPERIMENTAL PLATFORMS

Recently, we have designed and built two autonomous mobile manipulation platforms (Fig. 5). The Stanford Assistant Mobile Manipulator(SAMM) platforms have been developed in collaboration with Nomadic Technologies and Oak Ridge National Laboratories.

Each platform consists of a PUMA 560 arm mounted on a holonomic mobile base (Fig. 6). The PUMA manipulator is equipped with a 6-axis force sensor on the wrist, and an electric two-fingered gripper. The base consists of three "lateral" orthogonal universal-wheel assemblies that allow the base to translate and rotate holonomically in relatively flat office-like environments.[16] The base houses two personal computers, the motor amplifiers for both the base and arm, and batteries for approximately two hours of autonomous operation. In addition, a 1500 Watt AC power supply is included for tethered operations. Selection between on-board and tethered operations can be made while the robot is in operation.

Environmental sensing is currently provided by 48 sonars divided into two rings encircling the base. Sonars in the upper and lower rings fire simultaneously to allow through cross-echoes. This allows the detection of objects even if they are located in the

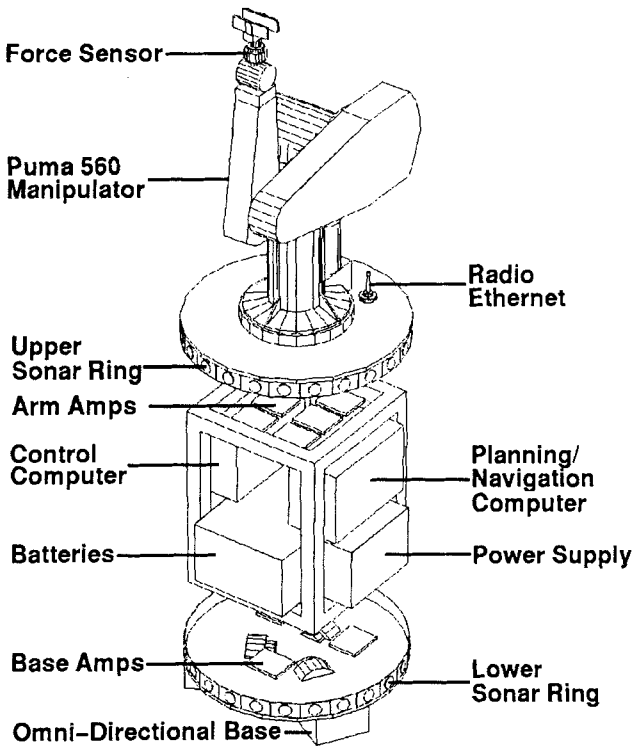


**Figure 6.** Platform components.

middle of the two sonar rings. We are currently working on adding vision capabilities to allow for more complex tasks.

The two personal computers with 90 MHz Pentium processors were selected over other competing technologies because of their relatively low cost and power consumption and the large selection of add-on cards. Also, this architecture will continue to be easily upgraded as computer technology advances.

The two computers in each robot are the heart of the multi-processing architecture. On each platform, one computer is devoted to robot control and other real-time tasks. The second computer is responsible for navigation, path planning, communication, and other less time-critical functions. Within the robot, the two computers communicate with each other through a wire Ethernet backbone.

Communication between robots or with other workstations is accomplished via a radio Ethernet link. This architecture is illustrated in Figure 7.

The control computer, running the real-time operating systems *VxWorks*, interfaces with the robot via an off-the-shelf, compact, modular multi-axis controller that provides 12 encoders channels, 16 D/A channels, and 8 A/D channels on a single EISA backplane slot. Information from the force sensor is received via a fiber optic link through a dedicated interface board at speeds of up to 1000Hz.

The navigation computer, running the *Linux* operating system, is responsible for tasks that do not require real-time performance. These include path planning and modification, environmental sensing, and communication with the other robots and the outside world. The sonar firing and timing is accomplished with a Motorola 6811 microprocessor board identical to the one used in the control computer. This frees almost all of this computer's processing power for planning, navigation, and self localization.

The control strategies discussed above have been successfully implemented in a system of two platforms. The dynamic coordination strategy has allowed full use of the relatively high bandwidth of the PUMA. Various tasks involving both free and constrained motions have been performed,[17] as illustrated in Figure 5. Object motion and force control performance with these mobile platforms are comparable with the results obtained with fixed base PUMA manipulators.

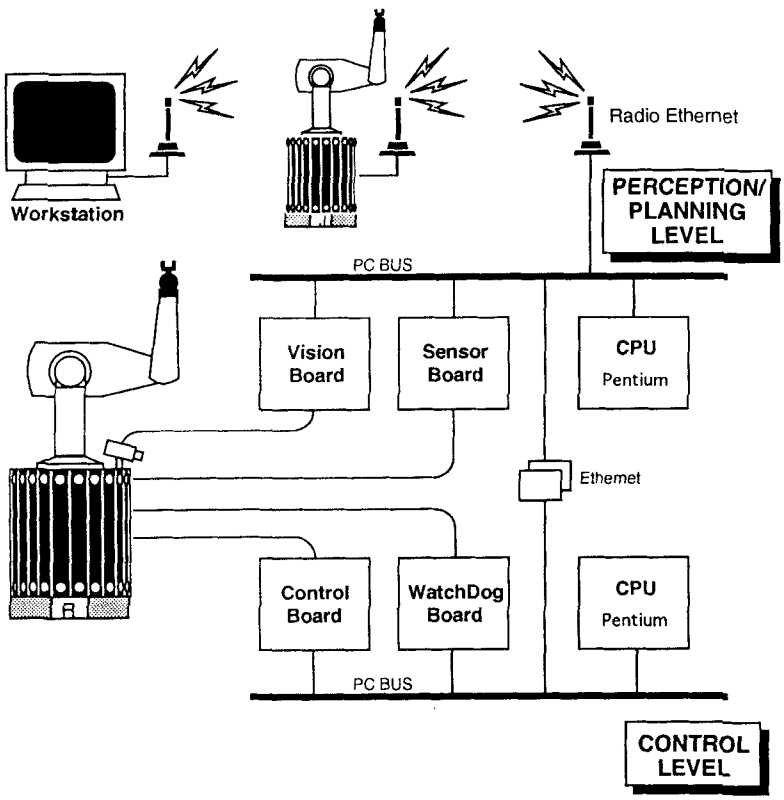


**Figure 7.** Platform computer architecture.

## 5. CONCLUSION

We have presented extensions of various operational space methodologies for fixed-base manipulators to mobile manipulation systems. A vehicle/arm platform is treated as a macro/mini structure. This redundant system is controlled using a dynamic coordination strategy, which allows the mini structure's high bandwidth to be fully utilized. For cooperative operations, we have developed a new decentralized control structure based on the *augmented object* and *virtual linkage* models that is better suited for mobile manipulator systems. Vehicle/arm coordination and cooperative operations have been successfully implemented on two mobile manipulator platforms developed at Stanford University.

The financial support of Boeing, General Motors, Hitachi Construction Machinery, and NSF (grants IRI-9320017 and CAD-9320419) is gratefully acknowledged. Many thanks to Andreas Baader, Alan Bowling, Oliver Brock, Francois Pin, James Slater, John Slater, Stef Sonck, and Dave Williams, who have made significant contributions to the design and construction of the Stanford robotic platforms.

## REFERENCES

1. M. Ullman, and R. Cannon, "Experiments in global navigation and control of a free-flying space robot," *Winter Annu. Meet. Am. Soc. Mech. Eng.*, 1989, Vol. 15, pp. 37–43.
2. Y. Umetani, and K. Yoshida, "Experimental study on two-dimensional free-flying robot satellite model," *Proc. NASA Conf.*, Space Telerobotics, 1989.
3. E. Papadopoulos and S. Dubowsky, "Coordinated manipulator/spacecraft motion control for space robotic systems," *Proc. IEEE Int. Conf. Rob. Autom.*, 1991, pp. 1696–1701.
4. J. Russakow and O. Khatib, "A new control structure for free-flying space robots," *Int. Symp. Artif. Intell. Rob. Autom. Space*, 1992, pp. 395–403.
5. O. Khatib, "A unified approach to motion and force control of robot manipulators: The operational space formulation," *IEEE J. Rob. Autom.*, **3**(1), 43–53, 1987.
6. O. Khatib, "Inertial properties in robotics manipulation: An object-level framework," *Int. J. Rob. Res.*, **14**(1), 19–36, 1995.
7. Y. F. Zheng and J. Y. S. Luh, "Joint torques for control of two coordinated moving robots," *Proc. IEEE Int. Conf. Rob. Autom.*, 1986, pp. 1375–1380.
8. M. Uchiyama and P. Dauchez, "A symmetric hybrid position/force control scheme for the coordination of two robots," *Proc. IEEE Int. Conf. Rob. Autom.*, 1988, pp. 350–356.
9. S. Hayati, "Hybrid position/force control of multi-arm cooperating robots," *Proc. IEEE Int. Conf. Rob. Autom.*, 1986, pp. 1375–1380.
10. T. J. Tarn, A. K. Bejczy, and X. Yun, "Design of dynamic control of two cooperating robot arms: Closed chain formulation," *Proc. IEEE Int. Conf. Rob. Autom.*, 1987, pp. 7–13.
11. J. A. Adams, et al., "Cooperative material handling by human and robotic agents: Module development and system synthesis," *Proc. IROS*, 1995, pp. 200–205.
12. O. Khatib, "Object manipulation in a multi-effector robot system," *Robotics Research 4*, R. Bolles and B. Roth, eds., MIT Press, Cambridge, MA, 1988, pp. 137–144.
13. D. Williams and O. Khatib, "The virtual linkage: A model for internal forces in multi-grasp manipulation," *Proc. IEEE Int. Conf. Rob. Autom.*, 1993, pp. 1025–1030.
14. D. Williams and O. Khatib, "Multi-grasp manipulation," *IEEE ICRA Video Proc.*, 1995.
15. O. Khatib, "Real-time obstacle avoidance for manipulators and mobile robots," *Int. J. Rob. Res.*, **5**(1), 90–98, 1986.
16. F. G. Pin and S. M. Killough, "A new family of omnidirectional and holonomic wheeled platforms for mobile robots," *IEEE Trans. Rob. Autom.*, **10**(4), 480–489, 1994.
17. O. Khatib, et al., "The robotic assistant," *IEEE ICRA Video Proc.*, 1996.